IR-visible upconversion and thermal effects in Pr^{3+}/Yb^{3+}-codoped Ga_2O_3:La_2S_3 chalcogenide glasses

2000 J. Phys.: Condens. Matter 12 10003

(http://iopscience.iop.org/0953-8984/12/48/316)

J. Phys.: Condens. Matter **12** (2000) 10003–10010. Printed in the UK PII: S0953-8984(00)14998-7

IR-visible upconversion and thermal effects in Pr^{3+}/Yb^{3+}-codoped Ga_2O_3:La_2S_3 chalcogenide glasses

P V dos Santos†, E A Gouveia†, M T de Araujo†, A S Gouveia-Neto†, S J L Ribeiro‡ and S H S Benedicto‡

† Departamento de Física, Universidade Federal de Alagoas, Maceió 57072/970, AL, Brazil
‡ Instituto de Química, UNESP, Araraquara, SP, Brazil

E-mail: artur@fis.ufal.br

Received 27 June 1999, in final form 5 September 2000

Abstract. IR–visible upconversion fluorescence spectroscopy and thermal effects in Pr^{3+}/Yb^{3+}-codoped Ga_2O_3:La_2S_3 chalcogenide glasses excited at 1.064 μm is reported. Intense visible upconversion emission in the wavelength region of 480–680 nm peaked around 500, 550, 620 and 660 nm is observed. Upconversion excitation of the Pr^{3+} excited-state visible emitting levels is achieved by a combination of phonon-assisted absorption, energy-transfer and phonon-assisted excited-state absorption processes. A threefold upconversion emission enhancement induced by thermal effects when the codoped sample was heated in the temperature range of 20–200 °C is demonstrated. The thermal-induced enhancement is attributed to a multiphonon-assisted anti-Stokes process which takes place in the excitation of the ytterbium and excited-state absorption of the praseodymium. The thermal effect is modelled by conventional rate equations considering temperature-dependent effective absorption cross-sections for the $^2F_{7/2}$–$^2F_{5/2}$ ytterbium transition and $^1G_4$–$^3P_0$ praseodymium excited-state absorption, and it is shown to agree very well with experimental results. Frequency upconversion in singly Pr^{3+}-doped samples pumped at 836 nm and 1.064 μm in a two-beam configuration is also examined.

1. Introduction

There has recently been an upsurge of interest in searching for new materials for application as hosts in IR–visible upconverters based upon rare-earth-doped optical glasses. Some of their many applications include: colour displays, high density optical data reading and storage, biomedical diagnostics, infrared laser viewers and indicators etc. The frequency upconversion process involves either sequential or multiphoton stepwise excitation and energy transfer between rare-earth ions in solids and subsequent emission of photons with energies higher than the excitation photons [1]. Among many host material alternatives, chalcogenide glasses [2] have emerged as promising contenders, owing to their low maximum phonon energy of $\sim$425 cm^{-1} [3], and high refractive index of $\sim$2.4 [2], which provide the necessary conditions for the realization of efficient optical amplifiers in the region of 1.3 μm [3] and upconversion lasers [4]. These characteristics, in association with the wide transparency region extending from 0.5 μm to 10 μm [2] of the chalcogenide glasses, have also led to the observation of new rare-earth transitions in the mid-infrared that cannot be obtained from silica or fluoride glass hosts [5, 6]. The suitability of chalcogenide glasses to be fibered has already been demonstrated [7, 8] and has also allowed the realization of a Nd^{3+}-doped gallium–lanthanum sulphide fibre laser [9]. However, for the majority of rare-earth single-doped systems the IR–visible

0953-8984/00/4810003+08$30.00

upconversion process has proven inefficient particularly for pumping in the wavelength region of 1.0 μm to 1.1 μm, where high power sources are commercially available. The realization of Yb^{3+}-sensitized materials which exploit the high absorption cross-section (peaked around 980 nm) of ytterbium, as compared to other rare-earth ions and the efficient energy-transfer [10] mechanism between pairs or triads of rare-earth ions, has allowed a substantial improvement in the upconversion efficiency in ytterbium-sensitized Tm^{3+} [11], Er^{3+} [12–14] and Pr^{3+} [15–18] doped bulk glasses and optical fibres. In this work, we report on the generation of intense blue–green to red light through frequency upconversion of 1.064 μm radiation in Pr^{3+}/Yb^{3+}-codoped Ga_2O_3:La_2S_3 chalcogenide glasses and thermally induced enhancement of IR–visible upconversion.

2. Experiment

The experimental investigation was carried out using 70% Ga_2O_3:30La_2S_3 chalcogenide glass samples singly doped with Pr^{3+} and doubly doped with Pr^{3+} and Yb^{3+}. The material presents good optical quality, is stable against atmospheric moisture, it exhibits low optical attenuation from 0.5 to 10 μm and, due to the low maximum phonon energy of $\sim$425 cm^{-1} [3], it is expected to present lower nonradiative decay rates as compared to fluorozirconate glasses with their maximum phonon energy of $\sim$590 cm^{-1}. The samples (singly or doubly doped) had the same concentration of 1000 ppm/wt of praseodymium ions and different concentrations of ytterbium ions (5000 (I), 8000 (II), and 11 000 (III) ppm/wt). The excitation sources were a cw Nd:YAG laser operated at 1.064 μm (Quantronix model 416) and a Ti:sapphire laser (Coherent model 890) tunable in the region of 710–890 nm. The pump beam was focused down into the samples by a 5 cm focal length lens and the pump beam waist at the samples location was $\sim$60 μm. The detection system comprized a scanning spectrograph with operating resolution of 0.5 nm equipped with an S-20 uncooled photomultiplier tube coupled to a lock-in amplifier and computer. The temperature of the samples was increased from 20 to 200 °C by placing it in an aluminum oven heated by resistive wire elements. A copper–constantan thermocouple (reference at 0 °C) attached to one of the sample's faces was used to monitor the temperature within $\sim$2 °C accuracy.

3. Results and discussion

In this section we present upconversion spectroscopy of praseodymium ions in glass for two pump configurations. In the first Pr^{3+}/Yb^{3+}-codoped samples are pumped at 1.064 μm and then a Pr^{3+} singly doped sample is pumped simultaneously by 836 nm and 1.064 μm light. Thermal effects on upconversion visible light emission in the Yb^{3+}-sensitized chalcogenide Pr^{3+}-doped sample is also examined in this section.

3.1. Upconversion spectroscopy

In a single-beam pump configuration at 1.064 μm, the Pr^{3+}/Yb^{3+}-codoped sample (I) presented a typical upconversion fluorescence emission spectrum such as the one depicted in figure 1. The spectrum presented in figure 1 exhibited distinct emission bands centred around 500, 550, 620 and 660 nm corresponding to the $^3P_0 \rightarrow {}^3H_4$, $^3P_0 \rightarrow {}^3H_5$, $^3P_0 \rightarrow {}^3H_6$+$^1D_2 \rightarrow {}^3H_4$ and $^3P_0 \rightarrow {}^3F_2$ transitions of Pr^{3+} ions, respectively. Pumping of the Pr^{3+} excited-state visible emitting levels is accomplished through a combination of multiphonon-assisted absorption of the Yb sensitizer, energy transfer and multiphonon-assisted excited-state absorption of the Pr acceptor, as portrayed in the energy-level diagram shown in figure 2(a). In a first step, a pump

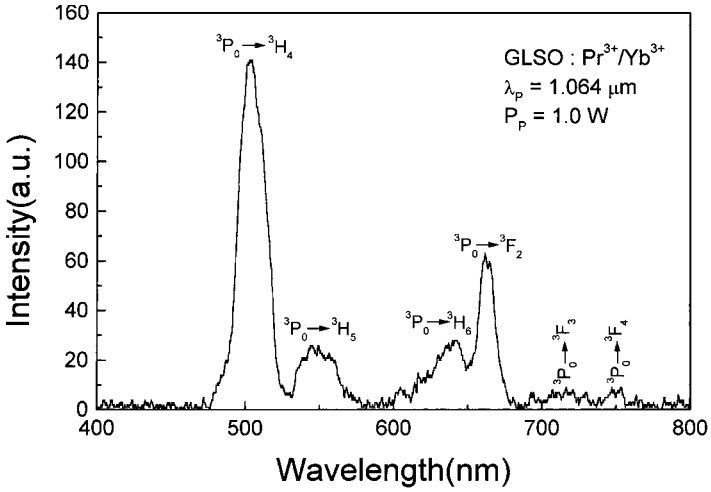

Figure 1. Frequency upconversion emission spectrum for the Pr^{3+}/Yb^{3+}-codoped sample (I) for an excitation power of 1.0 W at 1.064 μm at room temperature.

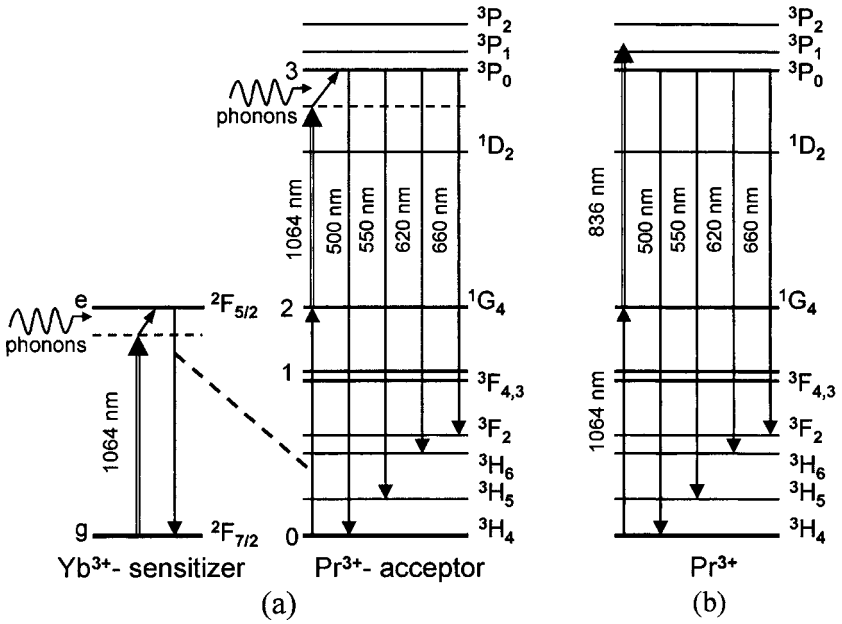

Figure 2. Energy-level scheme for (a) the Pr^{3+}/Yb^{3+} pair pumped at 1.064 μm indicating participation of phonons in the absorption transitions. The solid lines connected by a dashed line represent the cross-relaxation process. (b) Pr^{3+} excited in a two-beam configuration.

photon at 1.064 μm provokes a multiphonon-assisted anti-Stokes excitation of the Yb^{3+} sensitizer from the $^2F_{7/2}$ ground-state to the $^2F_{5/2}$ excited-state level. The excited Yb^{3+} transfers its energy to a neighbour Pr^{3+} ion in the $^3H_4$ ground state, exciting it to the $^1G_4$ level. This excited Pr^{3+} ion undergoes a multiphonon-assisted anti-Stokes excited-state absorption of a second pump photon, which promotes it to the $^3P_0$ upper emitting level. Finally, the excited Pr^{3+} ion decays from $^3P_0$ either radiatively to generate the main visible fluorescence emission bands

or nonradiatively to populate lower-lying luminescent levels, as indicated by the downwards arrows in figure 2(a). The dependence of the visible signals upon the excitation intensity at room temperature was examined and the results are presented in the log–log plot of figure 3. It was observed that all emission signals exhibited a quadratic power law behaviour (slope 2.2) with pump intensity. The deviation from the expected slope of 2.0 is within the experimental error of our measurements. These results corroborate our proposed upconversion pumping mechanism indicated in figure 2. Within the excitation power range (0.8–3.2 W) of our measurements, the results presented no evidence of an avalanche process [16] taking place as a possible upconversion excitation mechanism responsible for the population of the Pr^{3+} emitting levels. The avalanche process is characterized by a nonlinear dependence of the upconversion fluorescence emission upon the pump intensity with the existence of a critical pumping threshold [16, 19, 20]. The results did not reveal any onset of saturation effect either. For Pr^{3+} singly doped samples excited at 1.064 μm, no upconversion signal was observed even for pump powers as high as 3 W. However, we have performed measurements for Pr^{3+} single-doped samples in a two-laser-beam pump configuration, as indicated in the energy-level diagram of figure 2(b), and the visible upconversion fluorescence spectrum has shown identical features to the one obtained for the codoped samples. The upconversion excitation process for the double pumping configuration was achieved by a stepwise pumping process with ground-state followed by excited-state absorptions. At first, the Pr^{3+} ion in the $^3H_4$ ground state absorbs a 1.064 μm photon from the Nd:YAG laser, and is excited to the $^1G_4$ excited state. Then, the same Pr^{3+} ion in the $^1G_4$ excited state absorbs a 836 nm photon from the Ti:sapphire laser and is excited to the $^3P_{0,1}$ manifold and $^1I_6$ upper energy levels and, from there, the excited Pr^{3+} ion decays to generate the visible signals as indicated by the downwards arrows in figure 2(b). The Ti:sapphire laser was tuned to 836 nm providing maximum visible upconversion emission intensity. The upconversion fluorescence intensity as a function of excitation power was analysed and results are presented in the plots of figure 4. As can be inferred from data, indeed the upconversion signals presented a linear dependence on either of the laser intensities. It is important to point out that no upconversion signal was detected when either of the pump beams was blocked.

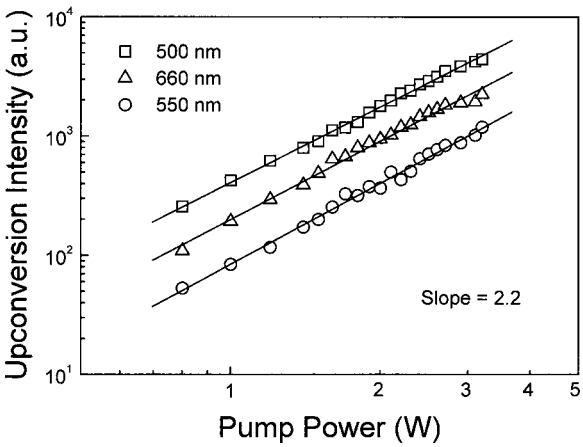

Figure 3. Log–log plot of the upconversion emission intensity for the main visible lines as a function of the excitation power at 1.064 μm for the Pr^{3+}/Yb^{3+}-codoped sample (I), at room temperature.

3.2. Thermal effects in Pr^{3+}/Yb^{3+}-codoped samples at 1.064 μm

The dependence of the upconversion fluorescence intensity for the Pr^{3+}/Yb^{3+}-codoped samples upon temperature was investigated for a fixed excitation power of 1.0 W at 1.064 μm, and the

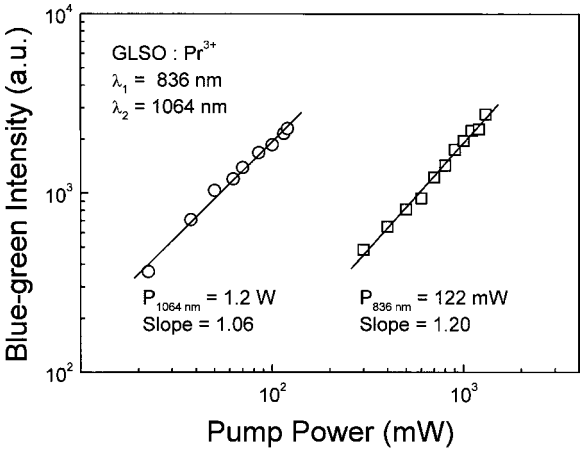

Figure 4. Log–log plot of the upconversion emission intensity for the blue–green line as a function of the excitation power for the singly Pr^{3+}-doped sample in the two-beam pump configuration, at room temperature.

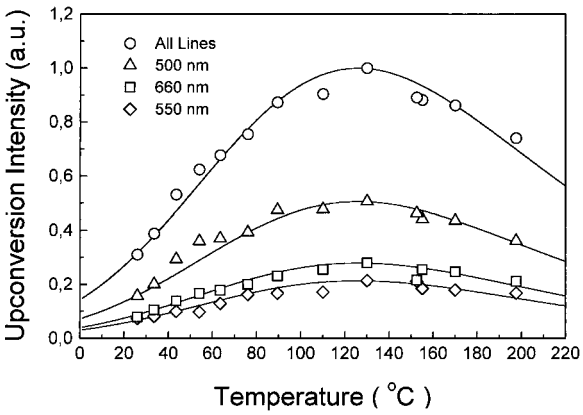

Figure 5. Temperature dependence of the visible upconversion emission signals for the Pr^{3+}/Yb^{3+}-codoped sample (I). Excitation power of 1.0 W at 1.064 μm.

results are presented in figure 5. As one observes, the upconversion visible fluorescence has enhanced by a factor of 3.3 in the temperature range of 20 to 200 °C. The 3.3 enhancement factor in the upconversion emission intensity was calculated by comparing the integrated visible spectrum at 130 °C and the one at room temperature (∼20 °C). The upconversion emission temperature behaviour can be explained as follows. The excitation of the Yb^{3+} sensitizer from the $^2F_{7/2}$ ground state to the $^2F_{5/2}$ excited state is accomplished through a multiphonon-assisted anti-Stokes excitation process [21] and requires the participation of two optical phonons in order to compensate for the energy mismatch of ∼800 cm^{-1} between the incident photon at 1.064 μm and the ytterbium transition energy. Furthermore, the praseodymium $^1G_4 \rightarrow {}^3P_0$ excited-state absorption also demands at least two optical phonons in order to match the energy difference of approximately 930 cm^{-1} between the pump-photon energy and that of the $^1G_4 \rightarrow {}^3P_0$ transition of Pr^{3+}. Accordingly, the population of the Pr^{3+} excited-state $^3P_0$ level relies strongly upon the phonon occupation number in the host matrix. The multiphonon-assisted absorption leads to temperature-dependent effective absorption cross-sections for both sensitizer and acceptor, which are increasing functions of the sample temperature yielding the enhancement of the populations of the emitting levels.

The temperature evolution of the main visible emission bands centered around 500, 550, 620 and 660 nm exhibited essentially the same behaviour, as shown in figure 5. The results are analysed using a model which includes a multiphonon-assisted transition in the Yb^{3+} ion

($^2F_{7/2} \rightarrow {}^2F_{5/2}$), energy transfer to Pr^{3+} ($^3H_4 \rightarrow {}^1G_4$) and subsequent phonon-assisted excited-state absorption from $^1G_4$ to populate the $^3P_0$ level as portrayed in figure 2(a). Accordingly, the temperature dependence of the population of the Pr^{3+} excited-state $^3P_0$ level is described by the following set of rate equations [22]:

$$\dot{n}_e = n_g \sigma_{ge}(T)\Phi - n_e C_{S2} n_0 - \frac{n_e}{\tau_S} \tag{1a}$$

$$\dot{n}_2 = n_e C_{S2} n_0 - n_2 \sigma_{23}(T)\Phi - \frac{n_2}{\tau_2} \tag{1b}$$

$$\dot{n}_3 = n_2 \sigma_{23}(T)\Phi - \frac{n_3}{\tau_3} \tag{1c}$$

where $n_e C_{S2}$ is the sensitizer–acceptor energy-transfer rate, τ_S, τ_2, and τ_3 are the lifetimes of the levels $^2F_{5/2}$ (level e), $^1G_4$ (level 2) and $^3P_0$ (level 3), respectively, and Φ is the power flux. In equations (1), $\sigma_{ge}(T)$ and $\sigma_{23}(T)$ represent the temperature-dependent effective absorption cross-sections for the Yb^{3+} excitation and Pr^{3+} excited-state absorption, respectively, owing to the so-called multiphonon-assisted anti-Stokes excitation process [21]. The absorption cross-sections can be written in a general form as

$$\sigma(T) = \sigma^0[\exp(h\nu_{phonon}/k_B T) - 1]^{-p} \tag{2}$$

where σ^0 is the absorption cross-section at resonance, $h\nu_{phonon}$ is the phonon energy, k_B is the Boltzmann constant and T the absolute temperature. The exponent p accounts for the number of phonons taking part in the anti-Stokes absorption processes. Combining the above equations, one obtains the steady-state population of the $^3P_0$ emitting level as

$$n_3 \cong \frac{\tau_2 \tau_3 \tau_S \sigma_{23}(T) N_A N_S C_{S2} \sigma_{ge}(T) \Phi^2}{(1 + \tau_S C_{S2} N_A)} \tag{3}$$

where N_A and $N_S = n_e + n_g$ are the Pr^{3+} and Yb^{3+} concentrations, respectively. In order to derive equation (3), we have assumed $\sigma_{23}\Phi \ll \tau_2^{-1}$ (fulfilled by our experimental conditions: $\tau_2^{-1} = 3700\ s^{-1}$ from [23] and $\sigma_{23}\Phi = 130\ s^{-1}$ at 1.064 nm for pump power of 2.7 W and σ_{23} from [24]), which implies that a small fraction of Pr^{3+} is excited, leading to $n_0 \approx N_A$. We have also neglected the term $\tau_S \sigma_{ge} \Phi$ in the denominator of equation (3) (which comes out since $n_g = N_S - n_e$) because it was observed that all visible emission lines exhibited an approximately quadratic power law behaviour (slope ~2) with pump intensity. The light intensity emitted of the $^3P_0$ level is then given by $I(^3P_0 \rightarrow i) = h\nu_{3i} A_{3i} n_3$, where A is the radiative transition rate from level 3 to the i level and ν_{3i} its frequency.

To obtain the temperature dependence of the emission intensity through equation (3) we need further considerations. The lifetime of the $^2F_{5/2}$ level is mainly radiative due to the large energy separation from the ground state (10 204 cm^{-1}). This means that the lifetimes τ_s is approximately temperature independent. Moreover, the energy-transfer rate $N_S C_{S2}$ is temperature dependent because of the energy mismatch ($\Delta E_{e2} = 164\ cm^{-1}$) between the $^2F_{5/2}$ level of Yb^{3+} and the $^1G_4$ level of Pr^{3+}, and this dependence can be accounted for through $\exp(-\Delta E_{e2}/k_B T)$ according to [21]. Finally, the lifetimes of the $^1G_4$ and $^3P_0$ are related to nonradiative transition probabilities $W^{NR}(T)$ through

$$\tau_i^{-1} = \sum_j A_{ij} + W_i^{NR}(T) \tag{4}$$

and for low concentrations of rare-earth ions, $W^{NR}(T)$ is due to multiphonon relaxation processes, and can be related to the temperature through [21, 22, 25]

$$W^{NR}(T) = W^{NR}(0)\lfloor 1 - \exp(-h\nu_{phonon}/k_B T)\rfloor^{-p} \tag{5}$$

where $W^{NR}(0)$ is its value at zero temperature and the exponent p is the phonon order linking the $^3P_0$ level (20 367 cm^{-1}) or $^1G_4$ level (10 040 cm^{-1}) to the next lower energy level.

Using, for our samples, the experimental lifetimes τ_2 ($\sim$264 μs), τ_3($\sim$4 μs) and nonradiative transitions rates $W_2^{NR}(300\ K) \cong 1827\ s^{-1}$, $W_3^{NR}(300\ K) \cong 50\,000\ s^{-1}$ for the levels $^1G_4$ and $^3P_0$, respectively, at room temperature [23], we have obtained the temperature dependence of the visible emission intensities of the $^3P_0$ level and the result is illustrated by the solids lines in the plot of figure 5. As can be observed, indeed the theoretical model matches very well the experimental results. By using a similar approach, we have recently described upconversion emission enhancement in Er^{3+}/Yb^{3+}-codoped chalcogenide bulk glass [26] and germanosilicate optical fibres [27], and the theoretical model based upon multiphonon-assisted anti-Stokes excitation of the nonresonant pumping of the sensitizer has also proven to agree very well indeed with the experimental data. Moreover, a model considering cooperative upconversion of Yb–Yb pairs as the major contribution to the upconversion pumping process of the Pr acceptor has also been tested but the resultant fitting has fallen far out from the experimental data. The theoretical fitting of data depicted in figure 5 also permitted us to withdraw the value of $\sim$320 cm^{-1} for the phonon mode participating in the multiphonon-assisted anti-Stokes excitation and excited-state absorption of the sensitizer and the acceptor, respectively. However, it can be inferred that there exists a deviation of $\sim$105 cm^{-1} from the value for the maximum phonon energy associated with chalcogenide glasses [3]. The deviation is attributed to the fact that in anti-Stokes sideband excitation processes [20], one has to consider an effective phonon mode, which possesses lower energy than the cut-off one. The phonon population distribution directly involved in the anti-Stokes excitation mechanism is centred around the so called 'effective phonon mode', as has recently been realized [28]. We have also performed the same set of experiments using samples II and III, and the results exhibited basically the same behaviour as far as visible emission temperature dependence is concerned. The upconversion emission efficiencies have followed the same trend with an overall maximum temperature enhancement of approximately $\times$3.0 for all samples. The emission spectra show the same profile as the one depicted in figure 1 for sample I. However, the samples II and III required pump powers of 750 mW and 350 mW, respectively, in order to obtain the same upconversion fluorescence signal level as sample I pumped with 1.0 W.

4. Conclusion

In conclusion, we have investigated IR–visible upconversion fluorescence spectroscopy in praseodymium single-doped Ga_2O_3:La_2S_3 chalcogenide samples in a double-pumping configuration and Pr^{3+}/Yb^{3+}-codoped samples excited at 1.064 μm. Thermally induced upconversion emission enhancement in Pr^{3+}/Yb^{3+}-codoped chalcogenide glasses excited at 1.064 μm was examined both theoretically and experimentally, for the first time. Our results have shown a threefold enhancement in the visible upconversion emission intensity as the temperature of the glass sample was varied in the 20–200 °C range. The temperature-induced upconversion emission enhancement was attributed to a temperature-dependent effective absorption cross-section for both the Yb^{3+}-sensitizer excitation and Pr^{3+}-acceptor excited-state absorption. The model based upon conventional rate equations, considering the absorption cross-sections of both sensitizer and acceptor as functions of the phonon population in the host matrix, has proven to agree very well with experimental data. Our results suggest that thermal enhancement processes can be exploited to improve power performance of Er^{3+}/Yb^{3+}-doped fibre lasers pumped by high-power sources in the 1.0 μm spectral region, and also enhance gain by 60% in a single-pass visible light amplification mechanism in Er^{3+}/Yb^{3+}-codoped chalcogenide glass pumped at 1.064 μm, as have recently been demonstrated elsewhere [29, 30].

Acknowledgments

The financial support for this research by FINEP (Financiadora de Estudos e Projetos), CNPq (Conselho Nacional de Desenvolvimento Científico e Tecnológico), CAPES (Coordenadoria de Aperfeiçoamento de Pessoal de Ensino Superior), PRONEX-UFPE/UFAL/UFPB and PADCT/CNPq, Brazilian agencies, is gratefully acknowledged. P V dos Santos was supported by a graduate studentship from CAPES.

References

[1] Auzel F 1973 *Proc. IEEE* **61** 758
[2] Kumta P N and Risbud S H 1994 *J. Mater. Sci.* **29** 1135
[3] Hewak D W, Medeiros Neto J A, Samson B, Brown R S, Jedrzejewski K P, Wang J, Taylor E, Laming R I, Wylamgowski G and Payne D N 1994 *IEEE Photon. Technol. Lett.* **6** 609
[4] Ye C C, Hempstead M, Hewak D W and Payne D N 1997 *IEEE Photon. Technol. Lett.* **9** 1104
[5] Wei K, Machewirth D P, Wenzel J, Snitzer E and Sigle G H Jr 1994 *Opt. Lett.* **19** 904
[6] Schweizer T, Hewak D W, Samson B N and Payne D N 1996 *Opt. Lett.* **21** 1594
[7] Ohishi Y, Mori A, Kanamori T, Fujiura K and Sudo S 1994 *Appl. Phys. Lett.* **65** 13
[8] Hewak D W, Moore R C, Schweizer T, Wang J, Samson B N, Brocklesby W S, Payne D N and Tarbox E J 1996 *Electron. Lett.* **32** 384
[9] Schweizer T, Samson B N, Moore R C, Hewak D W and Payne D N 1997 *Electron. Lett.* **33** 414
[10] Auzel F 1990 *J. Lumin.* **45** 341
[11] Hanna D C, Percival R, Perry I R, Smart R G, Townsend J E and Tropper A C 1990 *Opt. Commun.* **78** 187
[12] Hua Y-M, Li Q, Chen Y-L and Chen Y-X 1992 *Opt. Commun.* **88** 441
[13] Oliveira A S, de Araujo M T, Gouveia-Neto A S, Sombra A S B, Medeiros Neto J A and Aranha N 1998 *J. Appl. Phys.* **83** 604
[14] Oliveira A S, de Araujo M T, Gouveia-Neto A S, Sombra A S B, Medeiros Neto J A and Messaddeq Y 1998 *Appl. Phys. Lett.* **72** 753
[15] Baney D M, Rankin G and Chang K W 1996 *Appl. Phys. Lett.* **69** 1662
[16] Gosnell T R 1997 *Electron. Lett.* **33** 411
[17] Baney D M, Rankin G and Chang K W 1996 *Opt. Lett.* **21** 1372
[18] Lozano W B, de Araújo C B, Egalon C E, Gomes A S L, Costa B J and Messaddeq Y 1998 *Opt. Commun.* **153** 271
[19] Sandrock T, Scheife H, Heumann E and Huber G 1997 *Opt. Lett.* **22** 808
[20] Chivian J S, Case W E and Eden D D 1974 *Appl. Phys. Lett.* **35** 124
[21] Auzel F 1976 *Phys. Rev.* B **13** 2809
[22] Wright J C 1976 *Top. Appl. Phys.* **15** 239
[23] Hewak D W, Medeiros Neto J A, Samson B, Wang J, Tate H J, Pearson A, Brocklesby W S, Wylamgowski G, Laming R I, Payne D N, Jha A, Naftaly M, Jordery S and Poulain M 1993 *Optical Fiber Lasers and Amplifiers (SPIE)* vol 2073 (Bellingham, WA: SPIE) p 102
[24] Quimby R S and Zheng B 1992 *Appl. Phys. Lett.* **60** 1055
[25] Weber M J 1973 *Phys. Rev.* B **8** 54
[26] Dos Santos P V, Gouveia E A, de Araujo M T, Gouveia-Neto A S, Sombra A S B and Medeiros Neto J A 1999 *Appl. Phys. Lett.* **74** 3607
[27] Da Silva C J, de Araujo M T, Gouveia E A and Gouveia-Neto A S 2000 *Appl. Phys.* B **70** 185
[28] Auzel F and Chen Y H 1996 *J. Lumin.* **66/67** 224
[29] Da Silva C J, de Araujo M T, Gouveia E A and Gouveia-Neto A S 1999 *Opt. Lett.* **24** 1287
[30] Felix S F, Gouveia E A, de Araujo M T, Sombra A S B and Gouveia-Neto A S 2000 *J. Lumin.* **87–89** 1020